Conference Proceedings

EuroSun 2016
Palma de Mallorca (Spain), 11 - 14 October 2016

Theoretical Analysis of Vacuum Flat-plate Solar Collector with a Detailed Model

Viacheslav Shemelin[1,2], Tomas Matuska[1,2]

[1] University Centre for Energy Efficient Buildings, Czech Technical University in Prague

[2] Faculty of Mechanical Engineering, Czech Technical University in Prague

Abstract

Flat-plate collectors are generally designed for applications with typical working temperatures between 40 °C and 60 °C, which is mostly the case for domestic hot water systems. The major effect on the performance of flat solar collector has heat loss through glazing. The reduction of front side heat loss and consequently increasing efficiency can be achieved by using vacuum glazing. The paper presents a theoretical analysis of flat-plate solar collectors with a vacuum glazing. Different configurations of the collector have been investigated by a detailed theoretical model based on combined external and internal energy balance of the absorber. Performance characteristics for vacuum flat-plate collector alternatives have been derived. Subsequently, annual energy gains have been evaluated for a selected variant and compared with state-of-art vacuum tube collectors. The results of modeling indicate, that in case of using advanced vacuum glazing with special low-emissivity coating (emissivity 0.20, solar transmittance 0.85), it is possible to achieve efficiency parameters similar to or even better than vacuum tube collectors.

Keywords: *flat-plate collector, vacuum glazing, detailed model*

1. Introduction

Flat-plate solar collector (FPC) is the most widely used solar collector type in Europe. Simple structure, high optical efficiency, low cost, and safe operation are its main features. However, FPC is generally designed for a low temperature level between 40 °C and 60 °C, which is mostly the case for domestic hot water system. Any shifts to a higher temperature level could bring the extension of applicability range of FPC. Hence, efforts aimed to improve the performance of flat plate solar collectors are ongoing. The performance of a flat plate solar collector is largely influenced by the thermal losses from the absorber to the ambient via the transparent cover. One way to reduce this heat loss is to reduce the natural convection heat transfer in the space between the absorber and the cover by its partitioning with the use of additional glass pane, plastic film, or transparent insulation materials (TIM). Another way to reduce this heat loss is to use gas with lower thermal conductivity rather than air or by evacuating the space.

During the last 60 years a great number of research works have been done with the aim to develop new designs of solar flat-plate collector able to yield good performance at medium temperature range. The proposed designs are mainly centered around the objective to reduce heat losses, especially front side heat losses, e. g. by using transparent insulation materials (TIM), moderate vacuum, and high vacuum.

Veinberg and Veinberg (1959) investigated the use of “deep narrow meshes” as solar transparent honeycomb insulation. Further, Hollands (1965) presented the theoretical performance characteristics of a cellular honeycomb as a convection suppression device placed between the absorber and the outer glass cover of the FPC. Tabor (1969) presented a brief picture of cellular (honeycomb construction), indicating successful use of honeycomb insulation should wait for material with better physical properties and manufacturing technique. Later, Rommel and Wagner (1992) demonstrated that FPC containing 50-100 mm polycarbonate honeycomb

doi:10.18086/eurosun.2016.07.06 Available at http://proceedings.ises.org

layers function well with fluid working temperature between 40-80 °C. Higher working temperatures up to 260 °C are also possible using glass honeycombs, since plastic covers are susceptible to melting at temperatures above 120 °C. Svendsen and Jensen (1987) and Svendsen (1989) experimentally showed that solar FPC efficiency can be significantly improved by filling the air gap between absorber and cover with monolithic silica aerogel and evacuating to 10 kPa. Later, Duan (2012) studied the reduction of front side heat loss by placing the aerogel layer between the transparent cover and the absorber plate showing an increase of 21% in the collector efficiency respecting to the conventional collector.

However, most of the available transparent insulation materials are still not a good choice for high temperature flat plate collectors (Brunold et al., 1994). They either cannot withstand high temperature levels because they are made of plastics (most of honeycomb and capillary materials), they are hygroscopic and cannot withstand the humidity inside the collector (aerogels etc.), or they are very expensive (glass capillaries).

The use of a moderate vacuum in flate-plate collectors is known to reduce front side heat losses since the work of Eaton and Blumn (1975). The concept of an evacuated flat-plate collector was commercially realized and is available of the market. Apart from the higher thermal output, these collectors have the advantage of longer lifetime compared to nonevacuated collectors, because no humidity and condensation problems occur within the casing. Typical interior pressures, which can be maintained economically, lie between 1 and 10 kPa. It means that although convection losses are suppressed, gas conduction remains fully developed. Further, Benz and Beikircher (1997) constructed a prototype collector based on the commercially available flat-plate collector. To implement high thermal efficiency in the medium temperature range, the thermal losses of the absorber have been reduced using a low emissive selective absorber, a low pressure krypton filling (5 kPa) in the collector casing. The prototype collector has been dynamically tested and has showed very high efficiencies of more than 60% at 100 °C. Later Benvenuti (2005) presented a FPC, which is able to reach 300 °C. That has become possible by ultrahigh vacuum (1.33 x 10^{-7} Pa) maintained by a getter pump powered by the sun. After few years SRB Energy, with the support of CERN experts and facilities, has started the production of these collectors.

This paper presents the idea of replacing single glazing, which is used in most of flat solar collectors, with flat vacuum glazing, which, on the one hand, will show a low level of heat losses (low-emissivity coating, high vacuum) and, on the other hand, will demonstrate a high solar energy transmittance. Flat-plate solar collectors with low heat loss (at the level of vacuum tube collectors) and with a sufficiently high optical efficiency could be effectively used for integration into building envelopes (residential, industrial), which are widely available.

2. Vacuum glazing as a glazing cover of solar collector

Vacuum glazing consists of two glass sheets sealed together around the periphery. Glass sheets are supported by a pillar array arranged on a regular square grid pattern, and space between sheets is evacuated to a pressure lower than 0.1 Pa, thus effectively eliminating both gaseous conduction and convection. The pillars have a dimension of about 0.5 mm in diameter and behave like thermal bridges. Three different heat transfer mechanisms contribute to the total heat transfer coefficient $h_{g1\text{-}g2}$ of the glazing: thermal conduction through residual gas (h_{gas}), thermal conduction through spacers (h_{spac}), and radiation heat transfer between the two sheets (h_{rad}) in vacuum glazing. The total heat transfer coefficient $h_{g1\text{-}g2}$ between the glass sheets of a vacuum glazing can be approximated by the simple addition of individual heat transfer coefficients as (Weinlader et al, 2005; Collins and Simko, 1998)

$$h_{g1-g2} = h_{gas} + h_{rad} + h_{spas} = 0.8P + 4\varepsilon_{eff}\sigma T_{mean}^3 + \frac{2\lambda r}{d^2} \quad \text{(eq. 1)}$$

where P is internal pressure, σ is Stefan Boltzmann constant (5.67 x 10^{-8} W/(m^2.K^4)), T_{mean} is the average of temperatures T_1 a T_2 of the glass sheets, λ is the thermal conductivity of glass pillars, r is thr radius of glass pillars, d is the distance between pillars and, the effective emittance, ε_{eff}, is conventionally written as follows:

$$\varepsilon_{eff} = \frac{1}{\frac{1}{\varepsilon_1}+\frac{1}{\varepsilon_2}-1} \quad \text{(eq. 2)}$$

The relationship (eq. 1) is valid for the space with pressure less than 0.1 Pa, that is, high vacuum.

Vacuum glazing already appears in the portfolio of windows suppliers for use in buildings (Fig. 1). Commercially available vacuum glazing with configuration 3-0.2-3 mm has a transmittance of solar radiation of τ = 67 % and glazing center-of-glazing transmittance U value of 1.1 W/(m^2.K) (e.g. Pilkington Spacia).

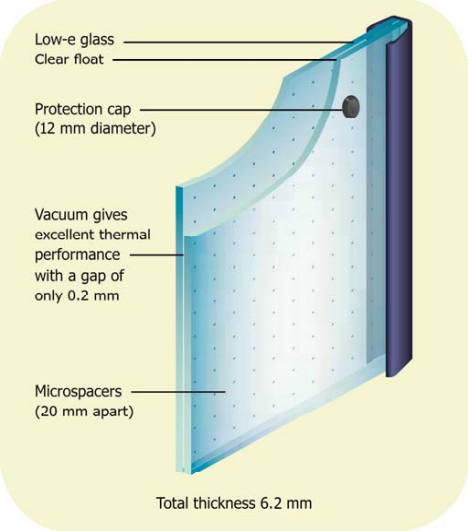

Fig. 1: Vacuum glazing (Pilkington Spacia)

Commercially available low-e coatings have been almost exclusively developed for architecture. To uphold the thermal and visual comfort in buildings, coating systems based on silver are primarily used, which can provide for extremely low emissivity (less than 0.03) and high visible transmittance (up to 0.90). Solar transmittance, however, is rarely higher than 0.60. A low solar energy transmittance, caused by reflectance of low-emissivity coating for the near infrared radiation (NIR) in the solar spectrum, is unsuitable for use in solar collectors. However, values up to 0.80 and corresponding higher emissivity (between 0.15 and 0.20) can be achieved using very thin silver layers, which have been developed in the last years for triple glazing, or with metal oxides (Fig. 2). It is also possible to use the external glass antireflection coatings on both surfaces and thus reduce reflection at the two boundary surfaces air-glass.

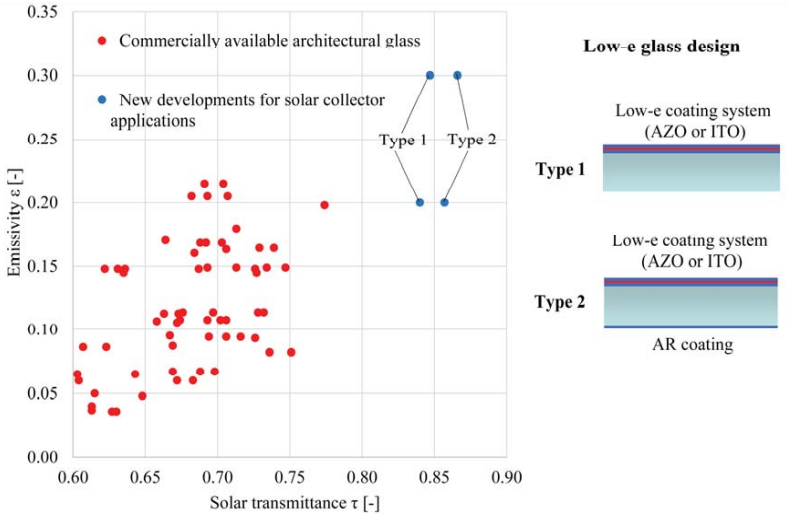

Fig. 2: Optical properties of spectrally selective glass with high solar transmittance for architecture and solar collector applications (Giovannetti et al, 2012)

To evaluate the potential of vacuum glazing application in solar thermal collector design, detailed simulations for three different variants of the collector cover glazing have been carried out. Reference variant (REF) is a simple solar low iron glass. The second variant (VG1) has a vacuum glazing based on two low iron glass without any coating. The last variant (VG2) is an advanced vacuum glazing with low-emissivity coating on

the outer surface of the inner glass (position 3). The optical properties of the coating are IR emissivity of 0.2 and solar transmittance of 0.85. Configurations of considered collector glazings are shown graphically in Fig. 3. The parameters of the cover glazings used for the comparative study are listed in Tab. 1.

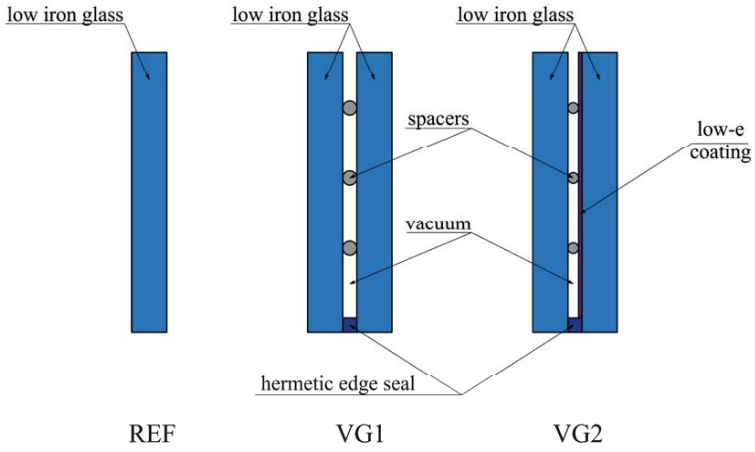

Fig. 3: Configurations of the investigated cover glazings

Tab. 1: Comparison of cover glazing physical properties

Properties	REF	VG1	VG2
Thickness of layers (mm)	4	4-0.2-4	4-0.2-4
Emissivity of surfaces (-)	0.85/0.85	0.85/0.85/0.85/0.85	0.85/0.85/0.2/0.85
Solar transmittance of glazing (-)	0.92	0.85	0.79

Since the thermal conductance is dependent on the temperature of the glazing, the heat transfer coefficient should be determined as a function of mean glazing temperature $T_{g1\text{-}g2}$ (Fig. 4)

$$h_{g1-g2} = f\left(T_{g1-g2}\right) = f\left(\frac{T_{g1}+T_{g2}}{2}\right) = h_{g0} + h_{g1}T_{g1-g2} + h_{g2}T_{g1-g2}^2 \qquad \text{(eq. 3)}$$

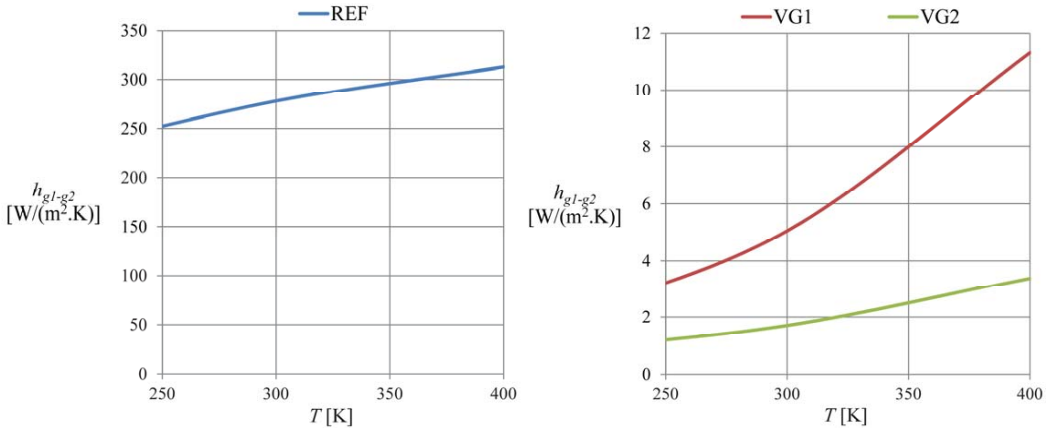

Fig. 4: Thermal conductance of the glazing as a function of mean temperature

3. Theoretical model of solar flat-plate collector

3.1. Description of the model

In order to analyze the thermal performance of FPC with considered variants of the transparent cover, a detailed theoretical model of the flat-plate collector Type 205 has been used and implemented into TRNSYS simulation software. The TRNSYS type is a successor of design tool KOLEKTOR 2.0 (Matuska and Zmrhal, 2009) originally developed as the Visual Basic program.

To compare the performance of given glazings the flat-plate collector has been considered consisting of an absorber placed in the insulated box covered with a given transparent cover. There is an air gap between the absorber and the cover and between the absorber and its back insulation, both defined by thickness and slope. The absorber is designed as a harp with distribution and riser pipes (defined by length, distance, and diameter). Transparent cover and back thermal insulation are defined by temperature dependent thermal conductance (see eq. 3).

The detailed model of flat-plate solar collector allows concluding a detailed calculation of heat transfer in the solar collector. Energy flow from the absorber surface to ambient and from the absorber surface to a heat transfer liquid, together with a temperature distribution in the collector, are calculated in the iteration loops. A solar collector can be specified by a number of detailed parameters, optical properties of glazing and absorber, and thermophysical properties of the main components of solar collector (frame, absorber, and transparent cover) in the model.

The implementation of the model in TRNSYS environment offers the parametric analysis for different construction alternatives for annual solar collector performance in the given solar system application. There is also a possibility to change a mathematical models describing the fundamental heat transfer phenomena (closed gap convection, wind convection, forced convection heat transfer in pipes etc.) and perform sensitivity analysis for selection of the models.

3.2. Basic equations

Mathematical model for solar flat-plate liquid collector solves one-dimensional heat transfer balances. Hottel and Woertz, Hottel and Whilier, and Bliss developed the simplest assumptions: thermal capacities, are neglected and a single value of collector overall heat loss coefficient is considered. Based on these assumptions and considering that the heat transfer is mainly one-dimensional and predominant in the direction normal to the absorber, Duffie and Beckman developed a simplified model (with electrical analogy) to characterize the solar collector in steady-state conditions.

The mathematical model in general consists of two parts: external energy balance of absorber (heat transfer from absorber surface to ambient environment) and internal energy balance of absorber (heat transfer from absorber surface into heat transfer fluid). The model solves the energy balance of the solar collector under steady-state conditions according to the principle Hottel-Whillier equation for usable thermal output

$$\dot{Q}_u = A_{abs} F_R [\tau_n \alpha_{abs} G_t - U(T_{in} - T_{amb})] \quad \text{(eq. 4)}$$

In this equation, A_{abs} is the absorber area, F_R is the collector heat removal factor, τ_n is the solar transmittance of the collector cover, α_{abs} is the solar absorptance of the absorber, G_t is the total solar irradiance, U is the overall heat loss coefficient of collector, T_{in} the inlet fluid temperature and T_{amb} is the ambient temperature.

The main planes of the collector are cover exterior surface (f_2), cover interior surface (f_1), absorber (abs), back insulation interior surface (b_1), back frame exterior surface (b_2), edge insulation interior surface (e_1), and edge frame exterior surface (e_2). A surface temperature is determined for each plane of collector during the calculation procedure. The main collector planes are schematically outlined in Fig. 5.

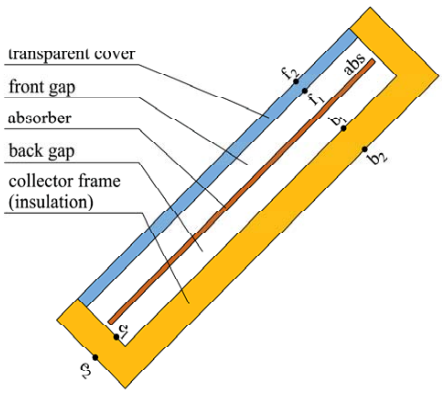

Fig. 5: Main temperature planes (surfaces) in solar collector model

Both external and internal energy balances are mutually dependent. The overall collector heat loss coefficient U as the main output from external balance is one of the inputs for internal balance. On the other side, mean absorber temperature T_{abs} as one of the outputs from internal balance is used as necessary input for external balance. Iteration loop has been introduced to transfer the results from external balance to starting internal balance and results from internal balance are put to external balance. Loop iterates as long as the difference between absorber temperatures calculated in two adjacent iteration steps higher than required minimum.

3.3. External energy balance

The external energy balance consists of:

- the heat transfer by radiation and by natural convection in the gap between absorber surface and transparent cover (respectively back insulation and edge insulation);
- the heat transfer by conduction through transparent cover (respectively back insulation and edge insulation);
- the heat transfer convection and radiation from exterior cover (respectively back frame and edge frame) surface to ambient.

To calculate the heat transfer coefficients properly (Fig. 6), temperatures for main collector planes (surfaces) should be known, but on the other side the temperature distribution in the collector is dependent on the heat transfer coefficients values. Therefore, external energy balance of absorber is solved in an iteration loop starting from first estimate of temperatures for each main surface based on given input temperature T_{in} and ambient temperature T_{amb}.

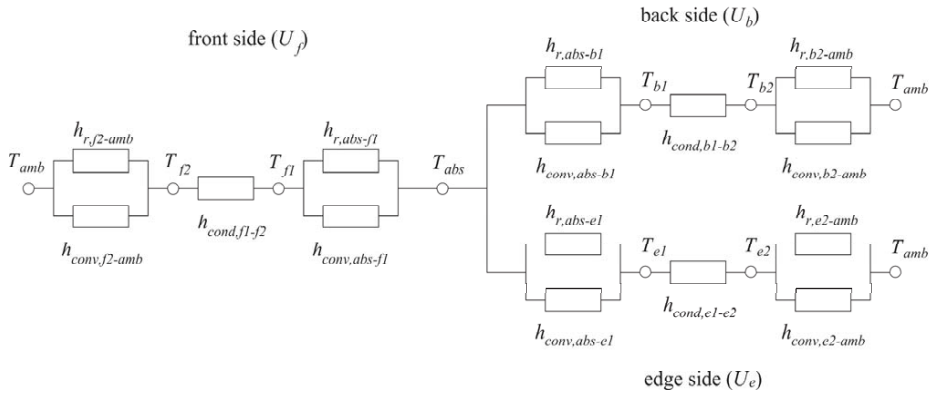

Fig. 6: Schematic detailed layout of external energy balance of absorber

3.4. Internal energy balance

The internal energy balance considers:

- the fin heat transfer by conduction;
- the heat transfer by conduction through the bond between absorber and pipes;
- the heat transfer by forced convection from interior surface of pipe to fluid.

Internal energy balance proceeds in its own iteration loop due to relationship between mean fluid temperature T_{mean} and forced convection heat transfer coefficients in absorber pipe register. The iterative calculation results of internal balance are collector efficiency factor F', collector heat removal factor F_R, usable thermal output and efficiency of solar collector.

3.5. Experimental validation

Type 205 has been experimentally validated in the frame of solar collectors testing according to European standard EN ISO 9806 in the accredited Solar Laboratory operated under University Centre for Energy Efficient Buildings, Czech Technical University in Prague. Solar thermal collectors have been tested to obtain steady state thermal output at constant operation conditions of inlet temperature (±0.05 K) and mass flow rate (±0.002 %) of heat transfer fluid (water) entering collector and at constant climatic conditions of solar irradiation (±1.4 %) and ambient temperature (±0.05 K).

Instantaneous efficiency has been calculated from collector thermal output related to total solar irradiation input (incident on collector reference area: gross area). Experimental data points of solar collector efficiency are coupled with uniform uncertainty bars in the graphs. Expanded uncertainty of efficiency and reduced temperature difference have been assessed for experimental data from both type A (statistical) and type B (instrumental) uncertainties considering the coverage factor k = 2 with 95% level of confidence (normal distribution).

The theoretical calculation of efficiency characteristic by the model is subjected to the uncertainty of input parameters. While geometrical parameters are easily available with high degree of confidence, the number of parameters defining the properties of collector parts is found uncertain within narrow range (e.g. absorber and glazing optical parameters, mostly ±2 %), middle range (e.g. conductivity of insulation layer dependent on its temperature and density, ±10 %), and quite broad range (e.g. emittance of absorber back side, insulation or collector frame, >10 %). Therefore, the results of theoretical calculation could be presented as two delimiting curves where the collector efficiency values can be found in reality.

The mathematical model has been validated in the field of atmospheric solar flat-plate collectors (top quality solar collectors with state-of-art copper laser welded absorber coated with a high performance selective coating and solar glazing as a transparent cover). Four different solar collectors have been used for detailed model validation. The majority of solar thermal collector parameters (e.g. thermal conductivity of insulation, the solar transmittance of the glazing, and the emissivity of the absorber) have been measured experimentally to reduce the uncertainty range. The model has also been tested in the case of various values of slope, mass flowrate, wind velocity, and incident radiation. More information about model validation could be found in (Shemelin and Matuska, 2015).

Fig. 7 shows experimentally measured efficiency points and theoretical modelled efficiency characteristics. It is evident from the results that simulated efficiency characteristics fit the measurements relatively well, which gives confidence about the developed model.

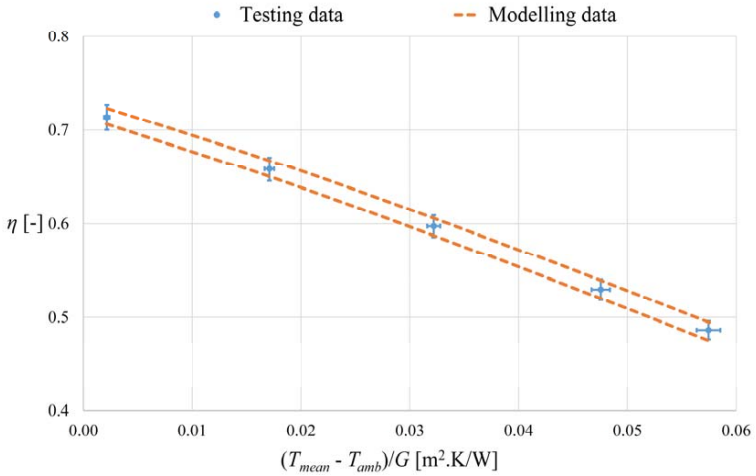

Fig. 7: Mathematical model validation

4. Results

Four configurations of FPC were modeled with dimensions 1 x 2 m. All variants have state-of-art copper laser welded absorber with a high performance selective coating with absorptivity of 0.95 and emissivity of 0.05. The thickness of the absorber is 0.2 mm and distance between pipes is 100 mm. Back thermal insulation and edge thermal insulation with thermal conductivity of 0.04 W/(m.K) have thickness 50 and 20 mm, respectively. The thickness of the air gap between absorber and glazing is 30 mm (except variant VC4, explained below). The difference between considered variants is only in the covering glazing.

The first configuration of FPC (RC) has a reference glazing (REF) as transparent cover with the parameters shown in Tab.1. The second configuration VC1 has a vacuum glazing VG1 instead of the reference glazing.

The third configuration VC2 considers variant VG2 as cover glazing. The last configuration VC3 has a principally different configuration. This variant has no gap between the absorber and the cover. Here, the absorber is bonded to the VG2 by permanently flexible, highly transparent silicone gel to reduce the whole thickness of the collector ("slim" collector alternative suitable for building envelope integration). Considered configurations of FPC collectors RC, VC1, VC2, and VC3 are shown in Fig. 8.

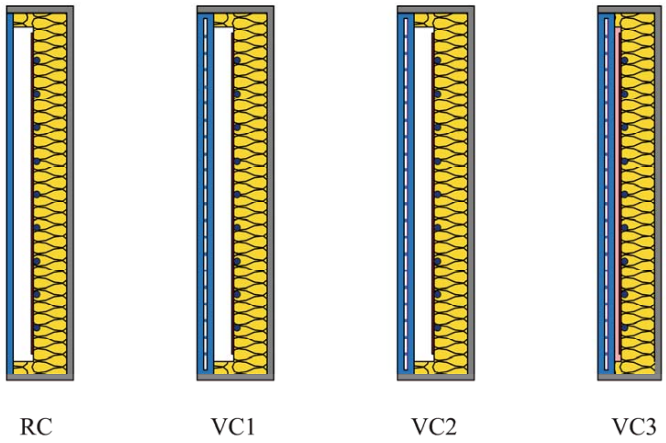

Fig. 8: Considered solar collector configurations

The graph in Fig. 9 shows the efficiency curves of considered solar collector variants. With respect to the EN ISO 9806 (2015) Standard "Solar energy-Solar thermal collectors-Test methods", the collector efficiency η is based on the collector gross area A_G. The calculations have been done with use of early described theoretical detailed model of FPC Type 205. The Graph shows the difference in energy quality of compared FPC variants. The low slope of the efficiency curve of the VC2 is due to the collector VC2 having two low-e coatings—the first inside the vacuum glazing and the second on the absorber surface. Other variants RC, VC1, and VC3 have only one low-e coating. Despite the vacuum layer, higher emittance of the glass low-e coating (0.2) in the VC3 variant instead of absorber coating with emittance 0.05 in the REF variant, brings the total top heat loss to similar value, but optical parameters of the VC3 configuration are lower (lower zero loss efficiency η_0). The resulting coefficients of efficiency characteristics η_0, a_1, and a_2 are listed in tab. 2.

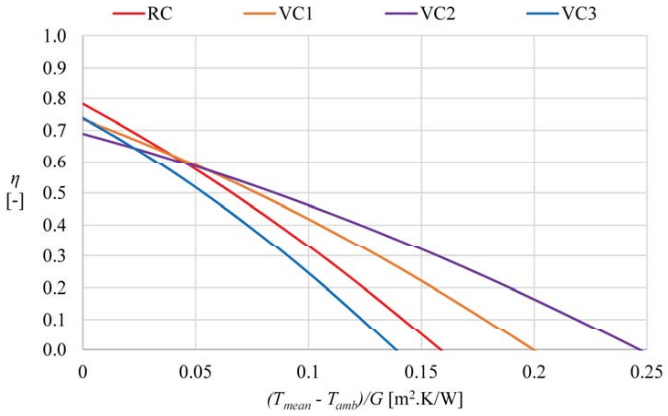

Fig. 9: Efficiency curves of different solar collector variants

Tab. 2: Summary of the collector simulation results

Collector variants	η_0 [-]	a_1 [W/(m^2.K)]	a_2 [W/(m^2.K^2)]
RC	0.783	3.788	0.006
VC1	0.734	2.634	0.004
VC2	0.689	1.919	0.003
VC3	0.738	3.890	0.009

On the other hand, solar collector variant VC3 has the lowest thickness between comparing variants – only 60 mm. Such thickness gives more possibility for integration of FPC into the building envelope because of the slim and compact design. Other variants RC, VC, and VC2 have thickness 87, 91 and 91 mm, respectively.

Fig. 10 presents the comparison of efficiency characteristics of flat-plate collector variant VC2 and vacuum tube collectors (with/without reflector, cylindrical/flat absorber) related to the gross area of collector. Thermal performance of solar flat-plate collector variant VC2 is comparable with that of vacuum tube collectors. Moreover, solar collector variant VC2 shows significantly higher efficiency than the majority of vacuum tube collectors (VT).

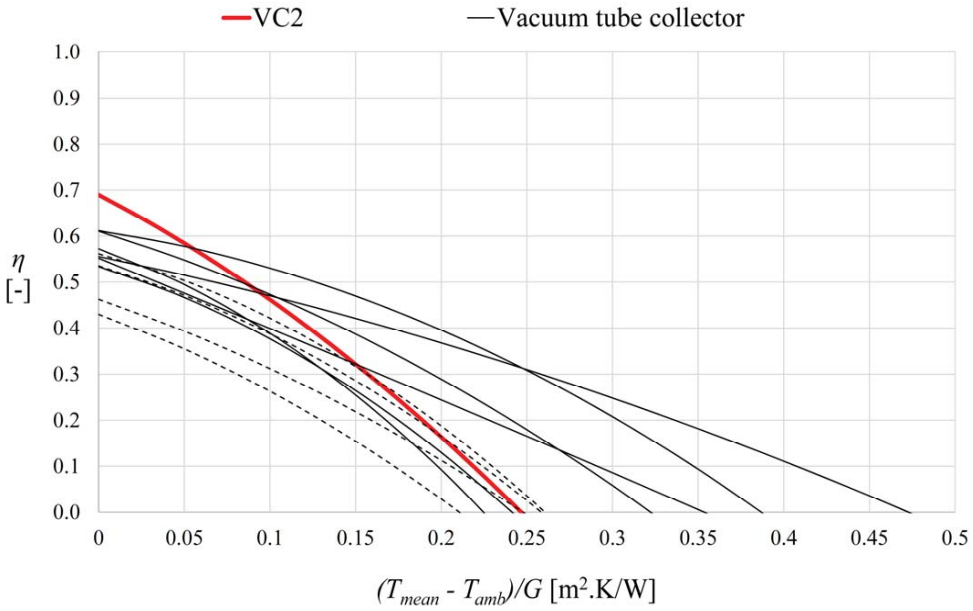

Fig. 10: Efficiency curves of different solar collector variants

To get a whole picture, the annual performance of the collector VC2 and VT collectors has been modelled using ScenoCalc software for constant operating temperatures 25, 50, 75, and 100 °C and climate conditions of Würzburg. The performance and optical characteristics of the compared collectors were used as input data. The results are shown in Tab. 3. The results of the modelling confirmed that the flat-plate solar collector variant VC2 has higher solar energy gains than the majority of vacuum tube collectors up to operating temperature 100 °C.

Tab. 3: Calculated annual solar collector gain with respect to the collector gross area

Solar gain [kWh/m^2]	25 °C	50 °C	75 °C	100 °C
VC2	697	548	422	320
VT1	653	**552**	**462**	**378**
VT2	586	480	386	303
VT3	527	465	390	308
VT4	603	511	421	**337**
VT5	616	515	416	320
VT6	577	478	386	304
VT7	**708**	**646**	**583**	**518**
VT8	607	493	400	318
VT9	626	**556**	**494**	**436**
VT10	667	**590**	**510**	**427**

5. Conclusions

Different designs of flat solar collectors based on a flat vacuum glazing have been theoretically investigated by using the detailed mathematical model to show the potential of vacuum glazing application in solar flat-plat collectors. The selected variant VC2 has been compared with state-of-the-art vacuum tube collectors by annual simulation of collector heat output in ScenoCalc. Results have shown, that there is a significant potential for increasing the efficiency of solar flat-plate collectors by using high performance vacuum glazing as a transparent cover. Collector variant VC2 shows higher performance than the majority of vacuum tube collectors up to operating temperature 100 °C.

Based on this analysis, now it is possible to proceed to the practical solution of the vacuum flat plate solar collector with vacuum glazing and low-emissivity coating (variant VC2). This collector promises to combine the low heat losses and the high solar energy transmittance.

6. Acknowledgment

This paper has been written with support by SGS16/212/OHK2/3T/12 - Modelling, control and design of environmental engineering installations.

7. References

Benvenuti C, 2005. Evacuable Flat Panel Solar Collector. PCT / EP 2004 / 000503. CERN.

Benz N., Beikircher T., 1999. High efficiency evacuated flat-plate solar collector for process steam production. Solar Energy Vol. 65, No. 2, 111-118.

Bliss J., 1959. The derivations of several “plate-efficiency factors” useful in the design of flate-plate heat collectors. Solar Energy Vol. 3, No. 4, 55-64.

Brunold, S., Frey, R., Frei, U., 1994. Comparison of three different collectors for process heat applications, Proceedings of SPIE – The International Society for Optical Engineering Optical Materials Technology for Energy Efficiency and Solar Energy Conversation XIII, Freiburg, Germany.

Collins, R. E., Simko, T. M., 1998. Current status of the science and technology of vacuum glazing. Solar energy Vol. 62, No. 3, 189-213.

Duan R., 2012. The efficiency of new solar flat-plate collectors. Advanced Materials Research, Vols. 347-353, 1337-1341.

Duffie J. A., Beckman W. A., 2006. Solar engineering of thermal processes, third ed., Wiley.

Eaton C., Blum H. A., 1975. The use of moderate vacuum environments as a means of increasing the collection efficiencies and operating temperatures of flate-plate solar collectors. Solar energy Vol. 17, 151-158.

Hottel H., Whillier A., 1955. Evaluation of flate-plate solar collector performance, Transactions of conference on the use of solar energy, 74-104.

Hottel H., Woertz B., 1942. The performance of flate plate solar collector, Transactions of ASME, No. 64, 91-104.

Holllands K. G. T., 1965. Honeycomb devices in flat-plate solar collectors. Solar energy Vol. 9, 159-164.

Rommel M., Wagner A., 1992. Application of transparent insulation materials in improved flat-plate collectors and integrated collectors storages. Sol Energy, Vol. 49, 371–380.

ScenoCalc v.5.01. Solar Collector Energy Output Calculator – a program for calculation of annual solar collector energy output. Available on https://www.sp.se/en/index/services/solar/ScenoCalc/Sidor/default.aspx

Shemelin V., Matuska T., 2015. TRNSYS type 205 – Detailed Model of Flat-Plate Solar Collector. Available

on: http://users.fs.cvut.cz/tomas.matuska/?page_id=582

Svendsen S., 1992. Solar collector with monolithic silica aerogel. Journal of Non-Crystalline Solids Vol. 145, 240-243.

Svendsen S., Jensen K. I., 1987. Flat Plate Solar Collector with Monolithic Silica Aerogel, Proceedings of ISES World Congress, Hamburg, Germany.

Matuška T., Zmrhal V. A mathematical model and design tool KOLEKTOR 2.2 reference handbook. 2009.

TRNSYS 17, TRNSYS: Transient System Simulation Tool. Available on http://www.trnsys.com/

Veinberg B. P., Veinberg V. B., 1959. Optics in equipment for the utilization of solar energy, State Publishing House of Defense Industry, Moscow (1959) [English translation]

Weinlader, H., Ebert, H.-P., Fricke J., 2005. VIG – Vacuum Insulation Glass, Proceedings of IVIS – 7th International Vacuum Insulation Symposium, Zurich-Duebendorf, Switzerland.

8. Web references

Pilkington Spacia. Available on: http://www.pilkington.com/en-gb/uk/products/product-categories/thermal-insulation/pilkington-spacia